Int. J. Multiphase Flow Vol. 8, No. 1, pp. 21–32, 1982
Printed in Great Britain.

0301-9322/82/010021-12$03.00/0
Pergamon/Elsevier

EXPERIMENTAL INVESTIGATION OF BUBBLY LUBRICATED EXTERNALLY PRESSURIZED THRUST BEARINGS

M. F. KHALIL† and E. RHODES

Department of Chemical Engineering University of Waterloo Waterloo, Ontario, Canada.

(*Received* 19 *November* 1980, *in revised form* 18 *May* 1981)

Abstract—Experimental results are presented for a bubbly lubricated externally pressurized circular thrust bearing. The data consists of the measured radial pressure distribution together with the lubricant mass flow rate over a wide range of inlet pressure, air mass flow rate ratio, for an either stationary or rotating bearing.

It is shown that the air injection always improves the pressure distribution in the bearing and so can completely avoid the negative pressure generated due to rotational inertia. Also it is shown that the bearing load carrying capacity increases as the injected air mass flow increases, especially at high inlet pressure. The lubricant mass flow rate is reduced by the increase of air mass flow rate and by the decrease of bearing rotational speed.

Finally the experimental results described in this paper are in good agreement with the mathematical analysis, based on the homogeneous flow model presented previously.

INTRODUCTION

Bubbly lubricated oil bearings have recently been analytically investigated by numerous investigators (Tonder 1975, 1976, 1977; Khalil & Rhodes 1980). The analytical interest stems from the fact that the gas or air bubbles are often present in lubricating oils and at certain conditions phase separation occurs due to reductions in pressure generated inside the fluid film due to either high operating speeds or low supply pressure (Coombs & Dowson 1965).

Tonder (1975, 1976, 1977) presented theoretical analyses for the effect of entrapped air or gas bubbles on the performance of hydrodynamic bearings for different film shapes. He concluded that due to the compressibility of the gas bubbles density gradients are created in the lubricant. This density gradient is shown to improve the pressure generated in the bearing gap and consequently bearing load carrying capacity. Also for different types of bearing, the study indicated that the effect was beneficial, in terms of unaltered frictional power due to relative motion between bearing surfaces, increased load capacity and better cooling due to the increase in lubricant volume flow rate.

Recently Khalil & Rhodes (1980) presented a theoretical study on the effect of bubbly lubricants on externally pressurized circular bearings. It was seen that the air bubbles improved the bearing load carrying capacity, and avoided the cavitation that was expected due to the rotational inertia. In addition there was a decrease both in lubricant mass flow rate and the frictional power consumed in bearing rotation.

This paper summarizes results of experimental studies that were undertaken to confirm the theoretical model presented previously (Khalil & Rhodes 1980).

MATHEMATICAL MODEL

The mathematical description of the bubbly lubricated bearing is based on a two-phase flow model. Two differential equations for lubricant pressure and temperature are obtained using equations of continuity, momentum and energy for a homogeneous mixture. Additional relations used are equations of state for gas and liquid, and a relation incorporating the effect of air quality on mixture density and viscosity.

The solution of the mathematical model has been presented previously (Khalil & Rhodes 1980). It involves lengthy manipulations and will not be repeated here. The basic equations are:

†On leave from Mechanical Engineering Department, Alexandria University, Alexandria, Egypt.

Pressure

$$\frac{d^2p}{dr^2}+\left(\frac{1}{r}+\frac{1}{\rho}\frac{d\rho}{dr}-\frac{1}{\mu}\frac{d\mu}{dr}\right)\frac{d\rho}{dr}=0.3\rho\omega^2 r\left(\frac{2}{r}+\frac{2}{\rho}\frac{d\rho}{dr}-\frac{1}{\mu}\frac{d\mu}{dr}\right). \quad [1]$$

Temperature

$$\frac{dT}{dr}=\frac{2\pi rh^3\mu}{MC_p}\left[\frac{1}{3}\left(\frac{1}{2\mu}\frac{d\rho}{dr}\right)^2+\frac{9}{7}\left(\frac{\rho\omega^2 r}{12\mu}\right)^2-\frac{\rho\omega^2 r}{20\mu^2}\frac{d\rho}{dr}+\left(\frac{\omega r}{h^2}\right)^2\right]. \quad [2]$$

Mixture properties

$$\mu=\left(\frac{x}{\mu_a}+\frac{1-x}{\mu_l}\right)^{-1} \quad [3]$$

$$\rho=\left(\frac{x}{\rho_a}+\frac{1-x}{\mu_l}\right)^{-1} \quad [4]$$

Gas phase equation of state

$$\rho_a=(\rho+\rho_{at})/\bar{R}T \quad [5]$$

$$\rho_l=\rho_l(T) \quad [6]$$

$$\mu_l=\mu_l(T) \quad [7]$$

where p is the pressure, μ is the mixture viscosity, ρ is the mixture density, ω is the angular speed of rotation, r is the radial location, T is the absolute temperature and t is the temperature, M is the lubricant mass flow rate, g is the specific heat at constant pressure, h is the film thickness, x is the mass ratio of air injected into the liquid, $\bar{R}$ is the gas constant of air, p_{at} is the atmospheric pressure and N is the speed of rotation. Subscripts a indicates air, l indicates liquid, 1 is at the inlet supply hose, 2 at the recess edge, 3 at the outer radius of the bearing.

Equations [1]–[7] completely describe the pressure and temperature profiles (in differential form), for the bubbly lubricated bearing. It can be solved numerically by an iteration process using finite difference techniques with the appropriate boundary conditions. From the obtained pressure and temperature distributions, the bearing load factor "L_f" and lubricant mass flow rate "M" are obtained using:

$$L_f=\left(p_1\pi r_1^2+\int_{r_1}^{r_3} p\,2\pi r\,dr\right)/p_1\pi r_3^2 \quad [8]$$

$$M=\frac{\pi rh^3\rho}{6\mu}\left[0.3\rho\omega^2 r-\frac{dp}{dr}\right]. \quad [9]$$

The effect of air bubbles content on the bearing pressure distribution, load carrying capacity and mass flow rates for different values of recess radius, bearing speed can be calculated and it is concluded that:

(i) The pressure distribution and load carrying capacity improves with the air bubble content for stationary and rotating bearings.

(ii) The negative pressure generated through high speed rotating bearing is avoided using bubbly lubricant.

(iii). The lubricant mass flow rate decreases with the air bubble content.

The solid lines in figures 3–16 of this paper are solutions to this model using boundary conditions appropriate to a circular disc bearing in which one surface is stationary and the other is rotating while mixtures of air and water are injected at the centre flowing outwards in the radial direction.

DESIGN OF EXPERIMENT

The main objective of the experimental investigation was to verify the theoretical model for a bubbly lubricated bearing.

Two forms of parallel circular plate thrust bearings were investigated; one arrangement had a flat plane stationary surface and the other had a central recess in the lower rotating plate as shown in figure 1. Radial pressure distributions and lubricant mass flow rates were recorded for both bearing arrangements over a wide range of air contents. The general predictions of the earlier paper (Khalil & Rhodes 1980) were substantiated by the experimental results, but the best results were achieved only when the fluid inertia effects were reduced to a minimum. For this reason a relatively small film thickness, 100 μm, was maintained between the bearing faces for most of the experiments.

Incompressible fluid (water) was supplied to the centre of the upper stationary circular plate as shown in figure 1. The rotating lower plate was mounted on the vertical shaft of a Weissenberg Rheogoniometer. One hp three phase synchronous motor with a gear box was giving a range of output speeds from 0 to 450 rpm. The apparatus was instrumented to a record fluid-film thickness, rotational speed, torque, and axial thrust on the upper plate (bearing load). The upper plate was made of 14 cm Perspex disk with a central hole of diameter 4 mm for water injection, also through which a needle of 2 mm diameter discharged air at the centre. The mixing of air and water took place in the central region of the bearing gap (figure 1) and the lubricant mixture flowed outwards with an increasing area of flow. By visual observation the air bubble sizes were judged to be of the same order as the bearing gap. The plate was provided with nine holes arranged at different angles for pressure taps at known radial positions. The holes were 1 mm in diameter, made by drilling normally to the disk surface. Each pressure tap was connected to one of the U-tube manometers filled with mercury or carbon tetrachloride.

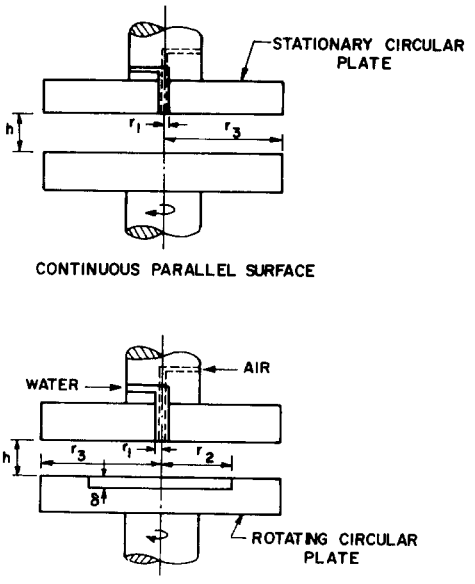

Figure 1. Externally pressurized bearing geometry.

Parallelism of the plates was ensured by monitoring the pressure from three pressure tapping points equispaced at 4.9 cm radius in the stationary bearing plate. The upper plate was adjusted until the three pressures were in closest agreement (normally within about 2%) and it was assumed that this agreement was an indication of the axial symmetry in pressure distribution and film shape.

Axial symmetry alone does not, of course, ensure that the bearing surfaces are parallel, but once the three test pressures were brought into agreement parallelism of the plate could be double checked by comparing the experimental and theoretical curve for pressure distribution using a single phase lubricant (water) for a stationary bearing.

The hydraulic circuit is shown schematically in figure 2. A 200 *l* stainless steel tank was filled partially with water and compressed air (above the water free surface) was introduced through a pressure regulating valve at constant pressure to ensure steady flow of water at constant-pressure to the bearing during the experiments. The water flowed from the tank through a flow control valve, filter, orifice meter, pressure regulator and needle valve, then to the supply hole in the upper plate. The air was introduced to the bearing through an air line consisting of flow control valve, orifice meter, pressure regulator and needle valve.

RESULTS

The data presented here are, of necessity, only a small number of those obtained during this series of tests. They are representative, however, and provide a sampling of the results of tests at various conditions. In all cases, performance characteristics were confirmed by repeat tests at the same operating conditions.

Pressure distribution

The pressure distribution for a bubbly flow lubricated stationary bearing is shown in figure 3 for different film thicknesses. It is clear from the figure that as the fluid gap increases the deviation between theory and experimental findings increases especially in the recess region (near the supply hole). This deviation is due to the omission of the fluid inertia effect in the mathematical model and it is more pronounced at higher lubricant velocities and consequently higher flow rates. The same phenomenon is observed in figure 4 for a rotating bearing. The two figures show that while deviation occurs in the recess region, a satisfactory agreement is obtained in the outer region (at larger radii).

Since the best agreement between theory and experiment was achieved only when the inertia effects were reduced to a minimum, a relatively small film thickness of 100 μm or less (which is similar to a real lubricating film) was investigated in the outer region for most of the experiments.

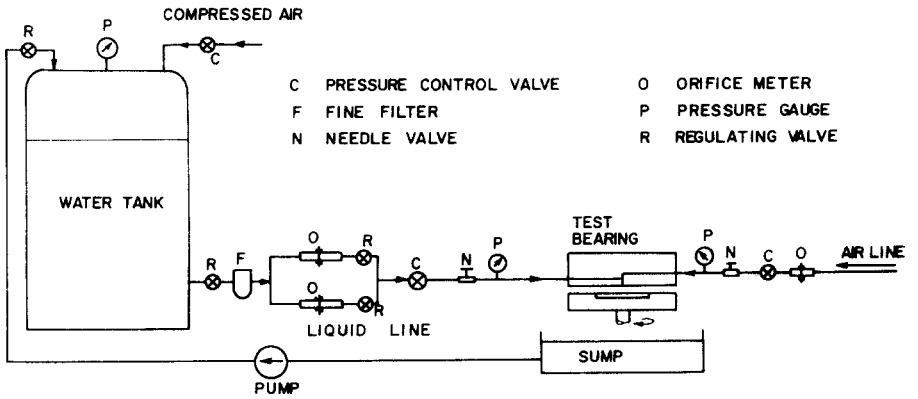

Figure 2. Hydraulic circuit.

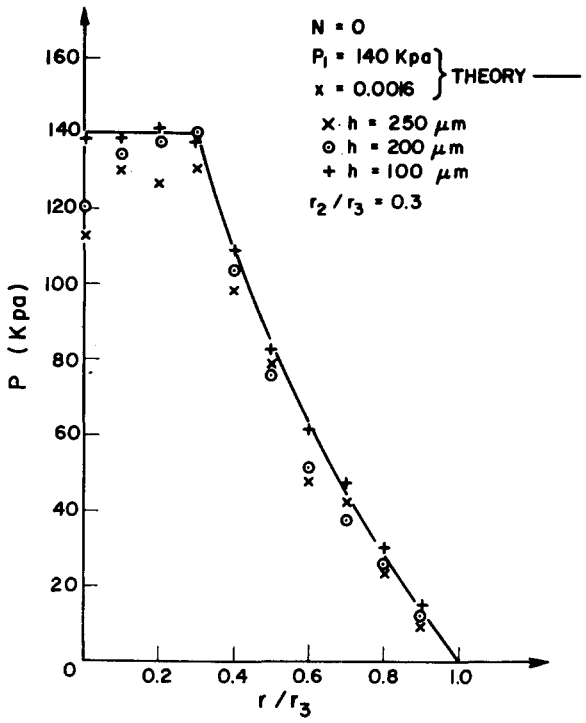

Figure 3. Effect of film thickness on pressure distribution of bubbly lubricated stationary bearing.

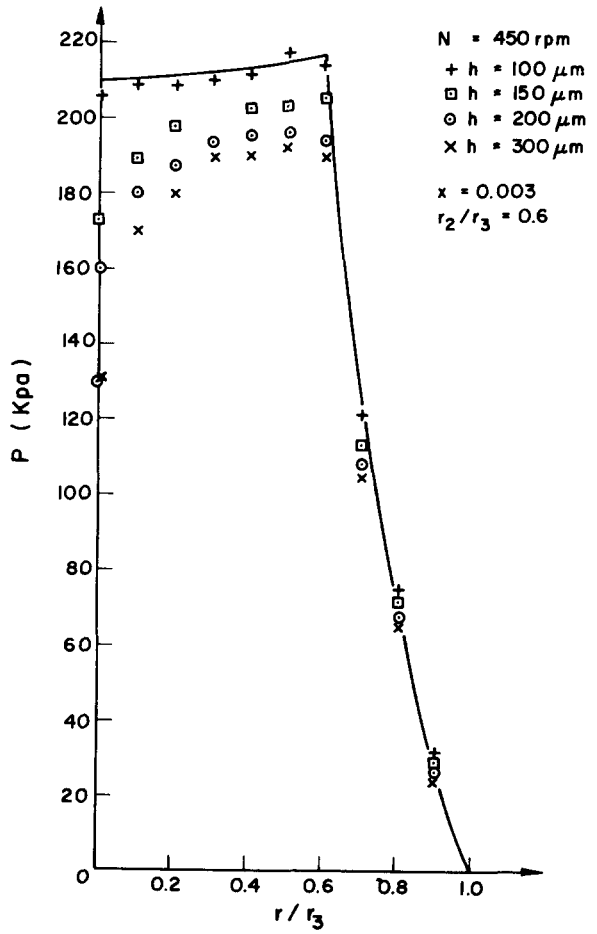

Figure 4. Effect of film thickness on pressure distribution of bubbly lubricated rotating bearing.

It is clear from both the pressure measurements (figures 5–16) and the theory that for an externally pressurized bearing, the pressure distribution over the bearing area is improved by injecting air through the incompressible lubricant. For a stationary non-recessed bearing (figure 5) the improvement of the pressure profile is increased as the percentage of the air injected increases. For the rotating bearing, figure 6 shows that by using pure lubricating liquid only, the pressure at any radius drops as the speed of rotation increases and the pressure at larger radii may fall below the ambient. The injection of air in this case improves the pressure situation and can avoid the negative pressure completely. Thus the injection of air can counteract the effect of rotation on the bearing load carrying capacity.

For a bearing with small recess size ($r_2/r_3 = 0.3$, figure 7) the pressure profile improves by injecting air through the lubricant especially at higher air mass flow rates.

For a rotating bearing using water only the pressure always rises in the recess region and the magnitude of this rise depends on the recess radius ratio (r_2/r_3) and speed of rotation (figures 8 and 10). Outside the recess region the pressures may fall or rise below the value corresponding to zero speed and thus may cause loss or gain in bearing load carrying capacity. For a recess radius ($r_2/r_3 = 0.3$) (figure 8), a considerable fall in pressure profile in the region outside the

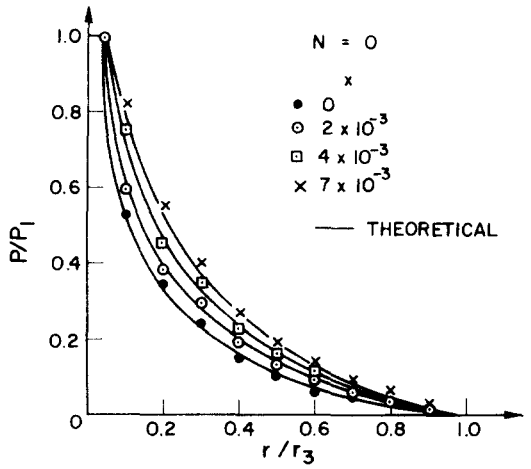

Figure 5. Effect of air content x on pressure distribution for nonrecessed bearing.

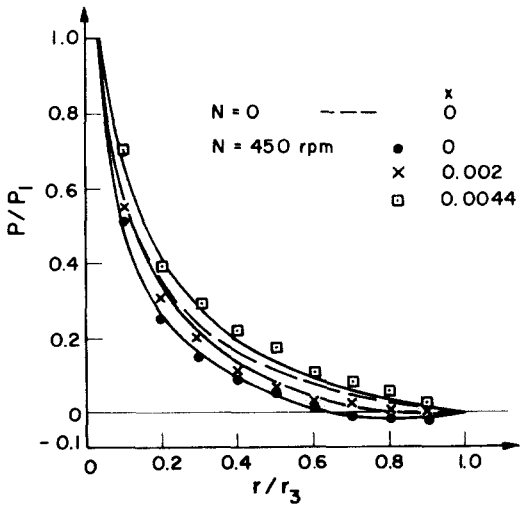

Figure 6. Effect of air content x on pressure distribution for rotating non-recessed bearing.

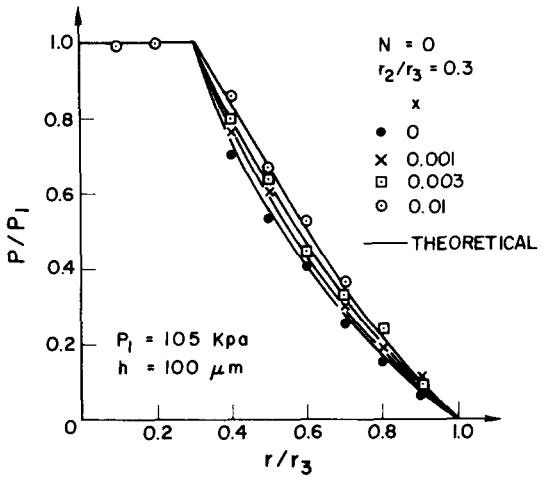

Figure 7. Effect of air content x on pressure distribution for stationary recessed bearing.

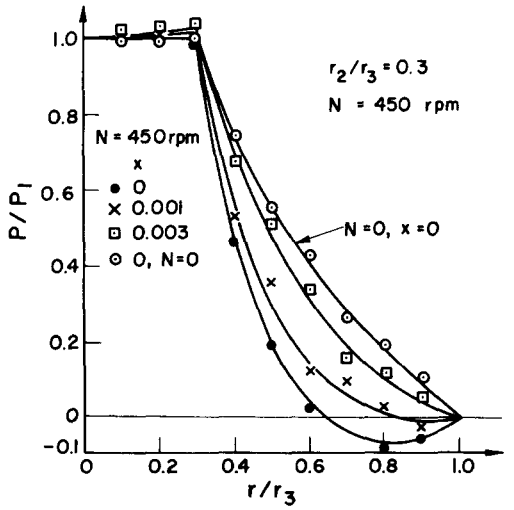

Figure 8. Effect of air content x on pressure distribution for rotating recessed bearing

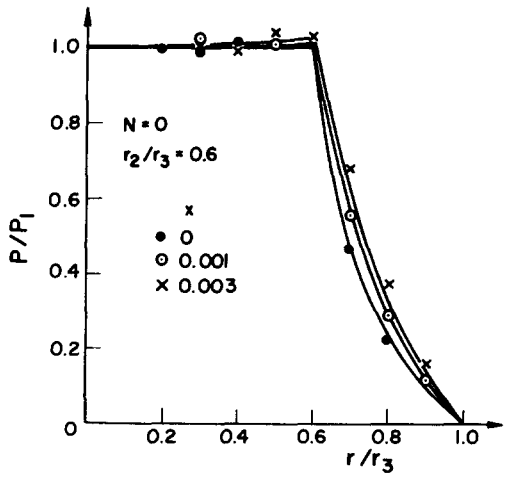

Figure 9. Effect of air content x on pressure distribution for stationary recessed bearing.

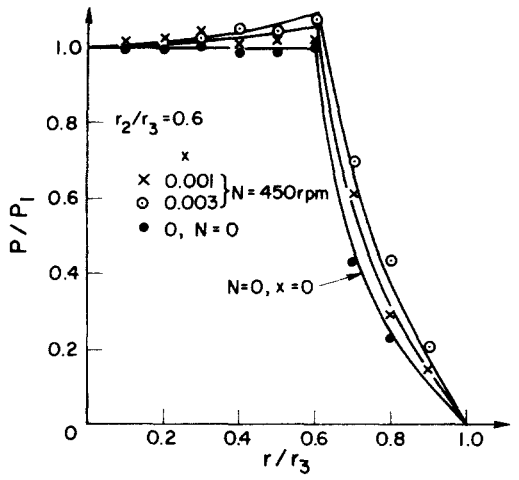

Figure 10. Effect of air content x on pressure distribution for rotating recessed bearing.

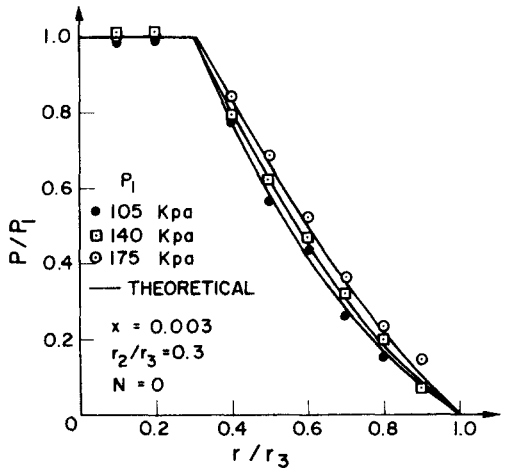

Figure 11. Effect of inlet pressure on pressure distribution of stationary bearing.

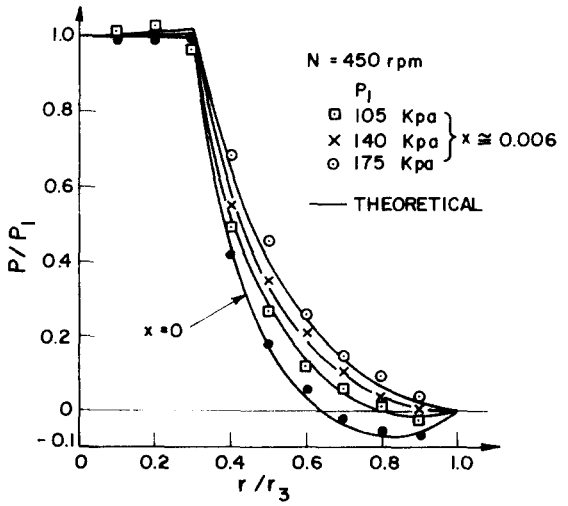

Figure 12. Effect of inlet pressure on pressure distribution of rotating bearing.

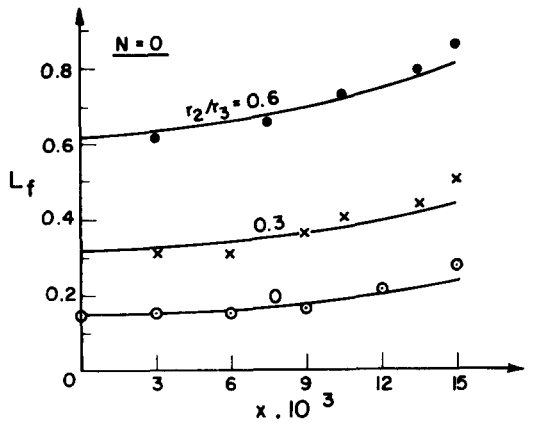

Figure 13. Effect of air content x and recess radius ratio on load factor.

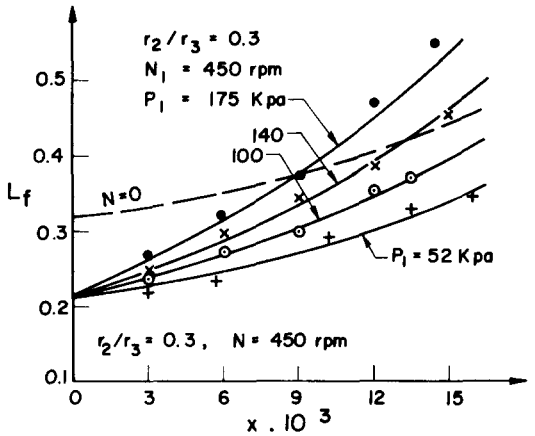

Figure 14. Effect of air content x and inlet pressure on load factor.

recess is observed and clearly indicates that the bearing rotation reduces the bearing load carrying capacity. For a larger recess radius ratio ($r_2/r_3 = 0.6$), figure 10 shows that the pressures are increased everywhere by rotation thus leading to an improvement in bearing load carrying capacity.

The injection of air through the bearing was seen to have an improving effect on the measured pressure distribution for both recess sizes and stationary or rotating conditions. Furthermore, the magnitude of negative pressure generated during rotation in the land region for bearings with small recesses could be reduced or avoided through air injection.

The effect of air injection on the dimensionless pressure distribution for a bearing with a recess radius ratio ($r_1/r_2 = 0.3$) is shown in figures 11 and 12 for different inlet pressures p_1. It is clear from the figure that as the inlet pressure p_1 increases the rise in pressure profile and bearing load also increases.

The pressure gain or drag reduction effect during the bearing operation may be explained in a qualitative manner. As the rate of injection of air into the lubricant, in laminar flow, is increased the fluid velocity rises and consequently the pressure drop along the bearing becomes greater. However if the mixture viscosity is sharply reduced, the pressure drop will decrease. The other effect of air injection is to reduce the wetted area of the bearing surface and in slug flow this area will be reduced approximately in direct proportion to the volumetric ratio of air to

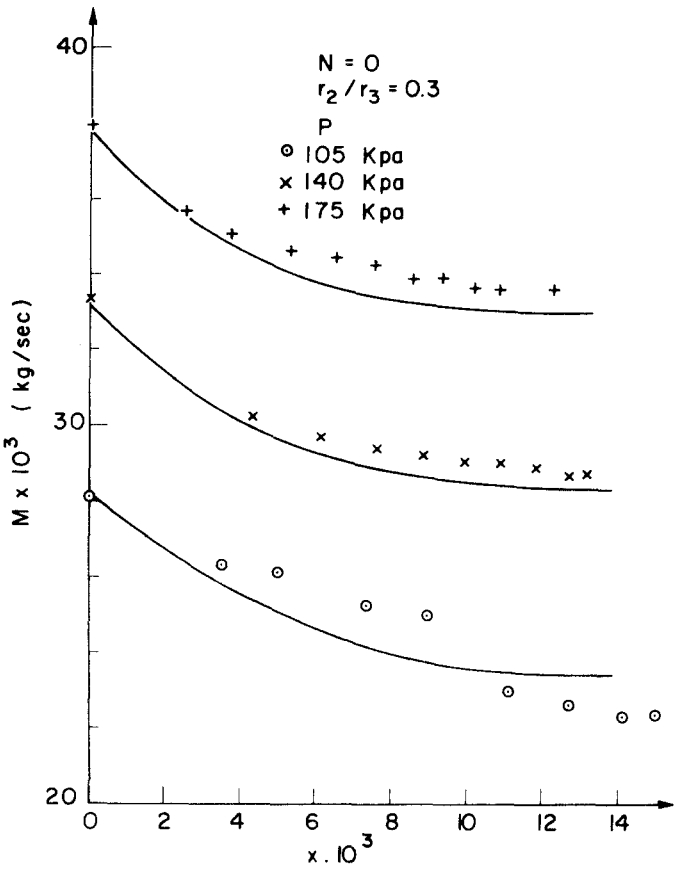

Figure 15. Effect of air content x and inlet pressure on lubricant mass flow rate for stationary bearing.

the liquid flow. If it is assumed that the pressure drop along the air slug can be neglected there will be a net improvement in the pressure profile over the bearing.

Bearing load carrying capacity

Due to some technical difficulties we cannot measure the bearing load carrying capacity directly, hence the records of the pressure distribution for the bearing under test are used to calculate the load factor "L_f" graphically using[8]. The effect of air injection and recess radius ratio on bearing load carrying capacity is shown in figure 13. In each case the experimental results are compared with the computed values using the previous analysis. It can be seen that the load carrying capacity is always improved by air injection and higher gain in load is obtained at a higher rate of air injection. Also figure 13 states that as (r_2/r_3) increases the bearing load carrying capacity increases.

The effect of bearing speed and air injection pressure on the load carrying capacity of bubbly lubricated bearing of recess radius $r_2/r_3 = 0.3$ is shown in figure 14. The figure indicates that at low air injection rates there is a reduction in the bearing load factor as bearing speed increases, whereas the reverse is true at high injection rates combined with high inlet pressures.

Lubricant mass flow rate

The effect of air injection ratio on the water mass flow rate through the bearing clearance is shown in figures 15 and 16. It is clear that the water flow rate increases as the inlet pressure p_1 increases, bearing rotational speed increases and as the air injection ratio decreases. The experimental values of mass flow rate were higher than the theoretical ones. This may be due to

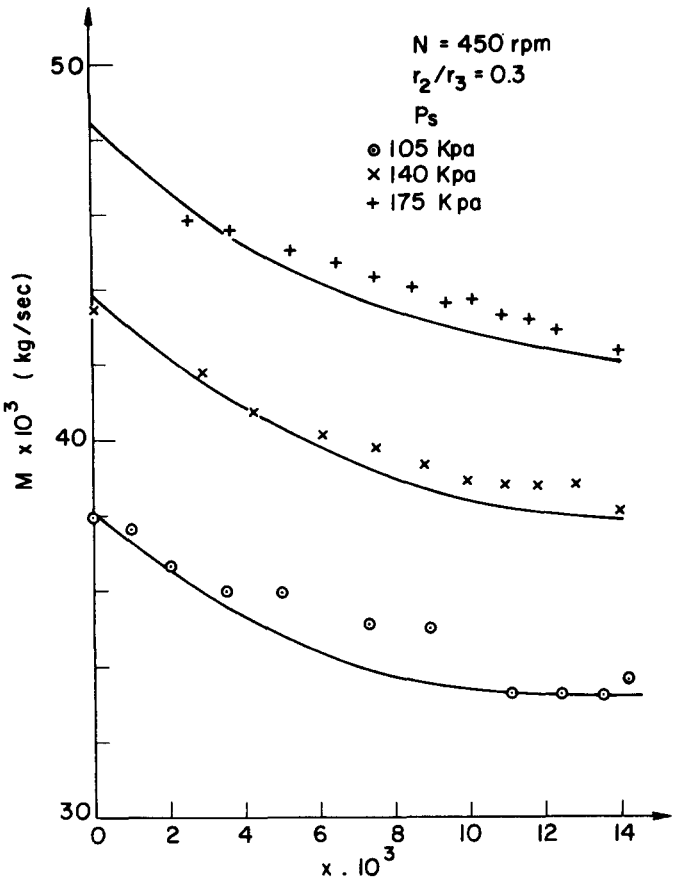

Figure 16. Effect of air content x and inlet pressure on lubricant mass flow rate for rotating bearing.

film thickness being higher than 100 μm during the bearing operation and also to the variation of water properties due to the slight variation in inlet temperatures.

CONCLUSIONS

It has been demonstrated both theoretically and experimentally that:

(1) The air injection always improves the pressure distribution and can avoid the negative pressure, due to rotational inertia, completely.

(2) The bearing load carrying capacity always increases as the percentage of air injected increases, especially at higher inlet pressure.

(3) The bearing load carrying capacity may increase or decrease by the bearing speed depending upon the bearing geometry.

(4) The lubricant mass flow rate decreases with the increase in air flow rate ratio and the decrease of both inlet pressure and bearing speed.

(5) Good agreement was observed especially at small film thickness between the experimental findings and the mathematical analysis based on the homogeneous flow model presented previously.

(6) When working at large film thickness, the effect of inertia due to fluid flow must be taken into account.

Acknowledgement—The authors are grateful to the Natural Sciences and Engineering Research Council Canada for the financial support of this research.

REFERENCES

COOMBS, J. A. DOWSON, D. 1955 An experimental investigation of the effects of lubricant inertia in a hydrostatic thrust bearing, lubrication and wear. *3rd Convention, Proc. Instn. Mech. Engrs.*, **179**, 96–108.

KHALIL, M. F. & RHODES, E. 1980 Effect of air bubbles on externally pressurized bearing performance. *Wear* **65**, 113–123.

TONDER, K. 1975 Effect on bearing performance of a bubbly lubricant. *JSLE-ASLE Int. Lubrication Conf. Tokyo*, Elsevier, Amsterdam, 1976.

TONDER, K. 1975 Parallel surfaces lubricated by a bubbly oil. *Wear* **35**, 23–24.

TONDER, 1976 Thermal model of effects of gas bubbles on the lubrication of parallel surfaces. *Wear* **40**, 37–50.

TONDER, K. 1977 Effect of gas bubbles on behavior of isothermal Michell bearings. *J. Lubrication Technology, ASME Trans.* **99**, 354–358.